

# Constraining neutrino masses with the ISW-galaxy correlation function

Julien Lesgourgues\* and Wessel Valkenburg†

*LAPTH, Université de Savoie & CNRS, BP110, F-64941 Annecy-le-vieux Cedex, France*

Enrique Gaztañaga‡

*Institut de Ciències de l'Espai, CSIC/IEEC, Campus UAB,  
F. de Ciències, Torre C5 par-2, Barcelona 08193, Spain*

(Dated: March 5, 2008)

Temperature anisotropies in the Cosmic Microwave Background (CMB) are affected by the late Integrated Sachs-Wolfe (IISW) effect caused by any time-variation of the gravitational potential on linear scales. Dark energy is not the only source of IISW, since massive neutrinos induce a small decay of the potential on small scales during both matter and dark energy domination. In this work, we study the prospect of using the cross-correlation between CMB and galaxy density maps as a tool for constraining the neutrino mass. On the one hand massive neutrinos reduce the cross-correlation spectrum because free-streaming slows down structure formation; on the other hand, they enhance it through their change in the effective linear growth. We show that in the observable range of scales and redshifts, the first effect dominates, but the second one is not negligible. We carry out an error forecast analysis by fitting some mock data inspired by the Planck satellite, Dark Energy Survey (DES) and Large Synoptic Survey Telescope (LSST). The inclusion of the cross-correlation data from Planck and LSST increases the sensitivity to the neutrino mass  $m_\nu$  by 38% (and to the dark energy equation of state  $w$  by 83%) with respect to Planck alone. The correlation between Planck and DES brings a far less significant improvement. This method is not potentially as good for detecting  $m_\nu$  as the measurement of galaxy, cluster or cosmic shear power spectra, but since it is independent and affected by different systematics, it remains potentially interesting if the total neutrino mass is of the order of 0.2 eV; if instead it is close to the lower bound from atmospheric oscillations,  $m_\nu \sim 0.05$  eV, we do not expect the ISW-galaxy correlation to be ever sensitive to  $m_\nu$ .

PACS numbers: 98.80.Cq

## I. INTRODUCTION

As photons pass through a changing gravitational potential well, they experience a redshift or a blueshift, depending on whether the well grows or decays respectively. Cosmic microwave background (CMB) photons can experience such variations between the time of last scattering and their detection now. This effect was first described by Sachs and Wolfe in 1967 [1], and hence is dubbed the integrated Sachs-Wolfe effect (ISW). During a Cold Dark Matter (CDM) and/or baryon dominated era, the gravitational potential distribution remains frozen, and the ISW effect has no net effect on the blackbody temperature of CMB photons. This property is crucially related to the fact that non-relativistic matter (like CDM and baryons) has a vanishing sound speed, and experiences gravitational clustering on all sub-Hubble scales after photon decoupling, as described by the Poisson equation. In such a situation, the universal expansion and the gravitational contraction compensate each other in such a way as to maintain a static gravitational potential. However, when the expansion rate is affected by any type of matter with a non-vanishing sound speed, e.g. during

Dark Energy (DE) domination, the gravitational perturbations decay and the cosmic photon fluid experiences a blue shift, acquiring extra temperature perturbations related to the intervening pattern of matter perturbations. It was first proposed by Crittenden and Turok in 1995 [2] to cross correlate maps of temperature perturbations in the CMB with those of matter overdensities in large scale structures (LSS), in order to measure a possible acceleration of the universe's expansion. However, the CMB and LSS data available at that time were not good enough for such an ambitious goal, and the first strong indication of a positive acceleration came in 1998 from the side of type-Ia supernovae [3, 4]. Analyses of the first (2003) and second (2006) data releases of the Wilkinson Microwave Anisotropy Probe (WMAP) [5, 6] were the first to indicate the existence of Dark Energy independent of acceleration, by means of the location of the second peak in the CMB power spectrum. Simultaneously, a number of interesting papers presented the first detections of the ISW effect by cross-correlating WMAP anisotropy maps with various LSS data sets [7, 8, 9, 10, 11, 12, 13, 14, 15], now able to give an independent measure for the acceleration of the expansion of the universe.

The domination of Dark Energy is not the only source of gravitational potential evolution and of a net ISW effect. On small cosmological scales, as soon as matter perturbations exceed the linear regime, gravitational perturbations start to grow and to redshift CMB photons. This effect, called the Rees-Sciama effect, has

\*Electronic address: julien.lesgourgues@lapp.in2p3.fr

†Electronic address: wessel.valkenburg@lapp.in2p3.fr

‡Electronic address: gazta@ieec.uab.es

not been significantly detected until now [16]. CMB photons can also be scattered by gravitational lensing [17] and by the Sunyaev-Zeldovich (SZ) effect [18] (see [9, 10, 19] for detections in CMB-LSS cross-correlation analysis). An other party expected to affect the evolution of gravitational perturbations –at least by a small amount– is the background of massive neutrinos. Over thirty years ago massive neutrinos were proposed as a Hot Dark Matter (HDM) candidate, and later ruled out as the dominant dark component, since HDM tends to wash out small scale overdensities during structure formation [20]. Observed neutrino oscillations however constrain neutrinos to have a mass [21, 22]. In addition, the presence of a Cosmic Neutrino Background (CNB) is strongly suggested on the one hand by the abundance of light elements produced during primordial nucleosynthesis [23, 24, 25], and on the other hand by CMB anisotropies [26, 27, 28, 29, 30, 31, 32, 32, 33, 34]. Therefore, a small fraction of HDM is expected to coexist with the dominant CDM component. On small cosmological scales (for instance, cluster scale), the free-streaming of massive neutrinos should induce a slow decay of gravitational and matter perturbations [35], acting during both matter and Dark Energy domination. This effect depends on the total neutrino mass summed over all neutrino families,  $m_\nu = \sum_i m_i$ , unlike laboratory experiments based on tritium decay or neutrinoless double-beta decay, which probe different combinations: hence, a cosmological determination of the total neutrino mass would bring complementary information to the scheduled particle physics experiments [37, 38]. The free streaming of massive neutrinos has not yet been detected [36], but there are good prospects to do so in the future, since the smallest total neutrino mass allowed by data on atmospheric neutrino oscillations ( $m_\nu \geq \sqrt{\Delta m_{\text{atm}}^2} \sim 0.05$  eV) implies at least a 5% suppression in the matter/gravitational small-scale power spectrum [37, 38]. A positive detection –even in the case of minimal mass– could follow from the analysis of future galaxy/cluster redshift surveys [39, 40, 41], weak lensing surveys [42, 43], Lyman- $\alpha$  forest analysis, cluster counts [40], etc. The goal of measuring the neutrino mass from cosmology is very ambitious since each of these methods suffers from its own source of systematics (bias issues, modeling of non-linear clustering, ...). Therefore, a robust detection could only be achieved by comparing the results from various types of experiments.

The goal of this work is to describe a possible cosmological determination of the absolute neutrino mass scale through the ISW effect induced by neutrino free-streaming on CMB temperature maps, using as an observable the cross-correlation function of galaxy-temperature maps. This possibility was investigated previously by Ichikawa and Takahashi [44] (and suggested again recently in [45]). As neutrinos slow down the growth of structure, we expect the blueshift caused by an accelerated expansion to be more pronounced if neutrinos have a larger mass. On the other hand, the distribution of matter inducing the late ISW effect is smoother

in case of free-streaming by massive neutrinos. These two antagonist effects should in principle induce some mass-dependent variations in the galaxy-temperature cross-correlation function.

In section II of this paper we give an outline of the theory of the ISW-effect in the presence of a neutrino mass. In section III, we use some mock data with properties inspired from the Planck satellite, Dark Energy Survey (DES) and Large Synoptic Survey Telescope (LSST) in order to show the potential impact of this method in the future.

## II. THE GALAXY-ISW CORRELATION IN THE PRESENCE OF NEUTRINO MASS

### A. Definitions

The observed galaxy overdensity  $\delta_G$  in a given direction  $\hat{n}$  is defined as

$$\delta_G(\hat{n}) = \int dz b(z) \phi_G(z) \delta_m(\hat{n}, z), \quad (1)$$

where  $z$  denotes redshift,  $b(z)$  is the redshift dependent bias function relating the observed galaxy overdensity to the total matter overdensity, and  $\phi_G(z)$  is the galaxy selection function which can be chosen such that only galaxies within a certain range of redshift are considered.

The observed CMB temperature map

$$\Delta_T(\hat{n}) \equiv \frac{T(\hat{n}) - T_0}{T_0} \quad (2)$$

results from various contributions, classified as primary or secondary anisotropies. By definition, secondary anisotropies are induced after photon decoupling and can be correlated to some extent with the surrounding large scale structure. The ISW component is one of these terms, and can be obtained by integrating the scalar metric perturbations (or just the Newtonian gravitational potential on sub-Hubble scales) along each line-of-sight between the last scattering surface and the observer. If the gravitational potential is written as a function of direction  $\hat{n}$  and redshift  $z$ , the ISW term reads

$$\Delta_T^{ISW}(\hat{n}) = -2 \int_0^{z_{\text{dec}}} dz \frac{d\Phi}{dz}(\hat{n}, z). \quad (3)$$

where  $z_{\text{dec}}$  is the redshift at decoupling. Immediately after decoupling and before full matter domination, the gravitational potential does vary with time: this is known as the early ISW (eISW) effect, in contrast with the late ISW (lISW) in which we are presently interested. The two maps  $\Delta_T^{eISW}$ ,  $\Delta_T^{lISW}$  can be computed separately by cutting the above integral in two pieces at some intermediate redshift  $z_*$  chosen during full matter domination, when the gravitational potential is static. Note that in presence of massive neutrinos, the potential is never really static on small scales, so the quantity  $\Delta_T^{lISW}$  might not be uniquely defined. Anyway,

this question is not relevant in practice. The observable quantity is not the late ISW auto-correlation function  $\langle \Delta_T^{ISW}(\hat{n})\Delta_T^{ISW}(\hat{n}') \rangle$ , but only its cross-correlation with a given survey  $\langle \Delta_T^{ISW}(\hat{n})\delta_G(\hat{n}') \rangle$ . Then, the redshift distribution  $\phi_G(z)$  selects the range in which the ISW effect is being probed, and the choice of  $z_*$  becomes irrelevant provided that  $z_*$  remains larger than the redshift of all objects in the survey:  $\phi_G(z_*) \simeq 0$ .

Assuming that the galaxy-temperature cross-correlation function arises solely from the late ISW effect (i.e., assuming that other secondary anisotropies potentially correlated with LSS can be separated or have a negligible amplitude, which is a good assumption on the scales considered hereafter), we can relate the galaxy-temperature correlation multipoles to the real-space correlation function  $\langle \Delta_T^{ISW}(\hat{n})\delta_G(\hat{n}') \rangle$ . In the Limber approximation (see Appendix), one gets

$$C_l^{TG} = \frac{3\Omega_m H_0^2}{(l+1/2)^2} \times \int_0^{z_*} dz b(z)\phi_G(z)H(z)a(z) \left[ \partial_z \frac{P(k, z)}{a(z)^2} \right]_{k=\frac{l+1/2}{r(z)}}, \quad (4)$$

where  $r(z)$  is the conformal distance up to redshift  $z$ ,  $H_0 = 100h$  km/s/Mpc is the Hubble parameter today, and the matter power spectrum is defined as  $\langle \delta_m(\vec{k}, z)\delta_m(\vec{k}', z) \rangle \equiv P(k, z) \delta^3(\vec{k} - \vec{k}')$ . Note that we used the Poisson equation in flat space in order to relate the gravitational potential  $\Phi$  to the matter overdensity  $\delta_m$ , and assumed  $a(0) = 1$  by convention. Finally, the multipoles  $C_l^{TG}$  define the angular correlation function in a Legendre polynomial basis ( $p_l$ ),

$$w^{TG}(\theta) = \sum_l \frac{2l+1}{4\pi} p_l(\cos\theta) C_l^{TG}. \quad (5)$$

Eq.(4) is often written in a form which assumes that the matter power spectrum is a separable function of wavenumber and redshift. This applies to the case of a (flat)  $\Lambda$ CDM universe, for which one can write

$$P(k, z) = D(\Lambda; z)^2 a(z)^2 P(k, 0) \quad (6)$$

with  $\partial_z D = 0$  during full matter domination and  $\partial_z D > 0$  during  $\Lambda$  domination. Figure 1 (left) shows the evolution of  $D$  as a function of  $z$  for  $\Omega_\Lambda = 1 - \Omega_m = 0.69$ . In the case of time-varying Dark Energy, the situation is qualitatively similar, and  $D$  just depends on more free parameters than  $\Lambda$ . In the rest of this paper, we will just write this function as  $D(z)$  for concision.

## B. Effect of neutrino masses

In models with massive neutrinos, the spectrum is not a separable function anymore (in other words, the linear growth factor is scale-dependent), and Eq.(4) cannot be further simplified. However, in order to make analytical estimates of the impact of neutrino masses on

$C_l^{TG}$ , it is possible to use some approximate solutions valid only on the largest and smallest wavelength (see [38] and [45] for more details). First, for wavelengths larger than the maximum value of the neutrino free-streaming scale, reached at the time of the transition to the non-relativistic regime, the power spectrum  $P^{f_\nu}$  is completely unaffected by neutrino masses, and identical to that in a massless neutrino model with the same cosmological parameters (in particular, the same  $\Omega_m$  and  $h$ ) noted as  $P^0$ :

$$\forall k < k_{nr}, \quad P^{f_\nu}(k, z) = [D(z)a(z)]^2 P^{f_\nu}(k, 0) \\ \text{with} \quad P^{f_\nu}(k, 0) = P^0(k, 0). \quad (7)$$

On the other hand, for wavelengths smaller than the free-streaming scale today, both the linear growth factor and the amplitude today are affected by neutrino masses, approximately like:

$$\forall k > k_{fs}, \quad P^{f_\nu}(k, z) \simeq [D(z)a(z)]^{2-\frac{6}{5}f_\nu} P^{f_\nu}(k, 0) \\ \text{with} \quad P^{f_\nu}(k, 0) \simeq [1 - 8f_\nu] P^0(k, 0), \quad (8)$$

where  $f_\nu = \Omega_\nu/\Omega_m$  stands for the neutrino density today relative to the *total* matter density (so  $\Omega_m$  includes baryons, hot and cold dark matter). Here  $D(z)$  is always the same function, computed either for  $f_\nu \neq 0$  on large scales, or for  $f_\nu = 0$  on any scale, with a common value of  $\Omega_\Lambda$  (or of Dark Energy parameters). The first approximation in Eqs. (8) is very accurate, as shown in Fig. 1 (left) where we compare the precise linear growth factor obtained numerically with the above solution. The second approximation is poorer, but more accurate ones can be found e.g. in Refs. [38, 45].

Assuming that the galaxy selection function is very peaked around a median redshift  $z_m$ , the multipole  $C_l^{GT}$  probes mainly fluctuations around the scale  $k \sim l/r(z_m)$ . If  $l$  is larger than  $k_{fs} r(z_m)$ ,  $C_l^{GT}$  is affected by neutrino masses through the term between brackets in Eq. (4). Using Eqs. (8), this term varies with  $f_\nu$  like:

$$\partial_z \frac{P^{f_\nu}(k, z)}{a(z)^2} \simeq [(1 + C(z)f_\nu)(1 - 8f_\nu)] \partial_z \frac{P^0(k, z)}{a(z)^2}, \quad (9)$$

$$\text{with} \quad C(z) = \frac{3}{5} \left( \frac{1}{1+z} \frac{D}{D'} - 1 \right).$$

For a typical Dark Energy model, the density fraction  $\Omega_{DE}$  becomes negligible for  $z > 2$  [55], and hence the ratio  $D'/D$  is tiny. So, at high redshift, the net effect of the neutrino mass is to increase the integrand in  $C_l^{TG}$  like:

$$\partial_z \frac{P^{f_\nu}(k, z)}{a(z)^2} \simeq \left[ \frac{3 f_\nu (1 - 8f_\nu)}{5} \frac{D}{1+z} \frac{1}{D'} \right] \partial_z \frac{P^0(k, z)}{a(z)^2}. \quad (10)$$

This just reflects the fact that at high redshift, the ISW effect would be null on all scales for  $f_\nu = 0$ , while for  $f_\nu > 0$  it is still active on small scales. However, for  $z < 2$ ,  $D'/D$  becomes larger, and for typical values of

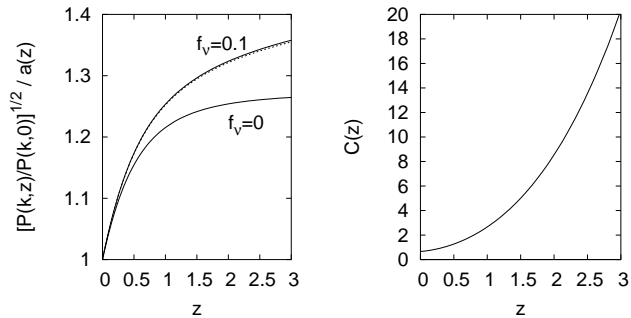


FIG. 1: (*Left*) Redshift evolution of the small-scale linear growth factor, defined here as  $[P(k, z)/P(k, 0)]^{1/2}/a(z)$  for  $k \sim 10 h\text{Mpc}^{-1}$ , and obtained numerically with CAMB for  $\Omega_\Lambda = 0.69$ . The lower curve corresponds to  $f_\nu = 0$  and is exactly equal to the quantity  $D(z)$  defined in Eq.(6). The upper, solid curve corresponds to  $f_\nu = 0.1$ , and is well approximated by the dotted curve, which corresponds to the first of Eqs.(8). (*Right*) The function  $C(z)$ , defined in Eqs.(9), computed here for  $\Omega_\Lambda = 0.69$ . Roughly speaking, the effect of neutrino masses on  $C_l^{TG}$  changes of sign when this function crosses eighth.

$\Omega_{\text{DE}} \sim 0.7$  there is always a redshift below which  $C(z)$  is smaller than eight. Then, the term between brackets in Eq. (9) is smaller than one, and the net effect of neutrino masses is to decrease  $\partial_z[P/a^2]$ . In Fig. 1 (right), we plot the function  $C(z)$  in the case of a cosmological constant with  $\Omega_\Lambda = 0.69$ . We see that  $C \sim 8$  for  $z \sim 2$ ; so, around this redshift and for  $l > k_{\text{fs}} r(z_m)$ , the net effect of neutrino masses on  $C_l^{GT}$  changes of sign.

In summary, if  $z_m$  is small, the expected effect of neutrino masses on the cross-correlation multipoles  $C_l^{GT}$  consists in a step-like suppression at large  $l$ 's, qualitatively similar to that observed in the galaxy auto-correlation multipoles  $C_l^{GG}$ . However the suppression factor is smaller, since the lack of power in the matter power spectrum caused by neutrino free-streaming is balanced by the excess of ISW effect due to the behavior of the linear growth factor in presence of massive neutrinos. When  $z_m$  increases, the boost related to the ISW effect is seen more clearly, and ultimately, when  $z_m$  is chosen before dark energy domination, the net effect of neutrino masses is to increase  $C_l^{GT}$  at large  $l$ .

In order to check and quantify these effects, we computed the cross-correlation multipoles  $C_l^{TG}$  (and also for comparison the auto-correlation multipoles  $C_l^{GG}$ ) for two different cosmological models, sharing the same parameters  $\Omega_b = 0.053$ ,  $\Omega_m = 0.31$ ,  $\Omega_\Lambda = 0.69$ ,  $h = 0.65$ ,  $A \equiv \ln[10^{10} k^3 \mathcal{R}^2]_{k=0.01/\text{Mpc}} = 3.16$ ,  $n_s = 0.95$ , but with two different values of the neutrino density fraction  $f_\nu = \Omega_\nu/\Omega_m$ , equal to 0 or 0.1 (corresponding to three neutrino species sharing the same mass  $m_\nu = 0$  or  $m_\nu \simeq 0.41$  eV). We adopted a galaxy selection function

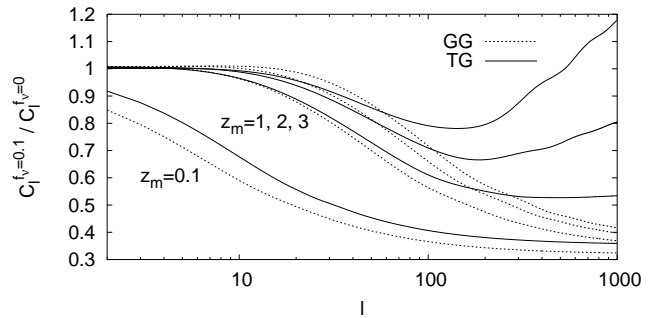


FIG. 2: Ratio of the cross-correlation multipoles  $C_l^{TG}$  and auto-correlation multipoles  $C_l^{GG}$  obtained for two cosmological models with neutrino density fractions equal to  $f_\nu = 0.1$  or 0, and the same value of other cosmological parameters (see the text for details).

of the form

$$\phi_G(z) = \frac{3}{2} \frac{z^2}{z_0^3} \exp \left[ - \left( \frac{z}{z_0} \right)^{\frac{3}{2}} \right], \quad (11)$$

peaking near the median redshift  $z_m \equiv 1.4z_0$ . For illustrative purposes, we choose the four values  $z_m = 0.1, 1, 2, 3$ , although in practice it would be very challenging to map  $\delta_G(\hat{n})$  for  $z \geq 2$ : presently, available data with a reasonable signal-to-noise ratio range only from  $z \sim 0.1$  to  $z \sim 1.5$ .

In Fig. 2 we plot the ratio of the multipoles  $C_l^{TG}$  in the two models, compared with the same ratio for  $C_l^{GG}$ . The free-streaming of massive neutrinos is responsible for the step-like suppression of  $C_l^{GG}$ , like in the power spectrum  $P(k)$ . The value of  $z_m$  controls the angle under which the free-streaming scale is seen in the map  $\delta_G(\hat{n})$ , and hence the scale at which the suppression occurs in multipole space. As expected from the previous discussion, the neutrino mass effect on  $C_l^{TG}$  is similar to that on  $C_l^{GG}$  for small  $z_m < 1$ , although the suppression factor is slightly smaller, due to the excess of ISW effect in presence of massive neutrinos. For  $z_m \geq 1$ , the amplification effect due to this excess has a clear and distinct signature at  $l \geq 100$ , and for  $z_m \sim 2$  the ratio displayed in Fig. (2) has a dip around  $l \sim 150$ . Unfortunately, we will see in Sec. II C that for  $l \geq 100$  this effect is masked by primary CMB anisotropies, which play the role of white noise for the present purpose.

In Fig. 3, we plot directly the multipoles  $C_l^{TG}$  for the same two models. The effect of neutrino masses is clearly visible for all  $l > 2$  at  $z_m = 0.1$ , while for  $z_m \geq 1$  it is necessary to reach  $l \geq 20$  in order to see a difference (since the maximum free-streaming scale is seen under a smaller angle at higher redshift). Remembering that the effect of neutrino masses on large  $l$ 's can be split in two contributions, a matter power suppression and an excess of ISW, it is clear from the previous discussion that the latter effect contributes at all redshifts, but its most obvious manifestation is the fact that  $C_l^{TG}$  increases with

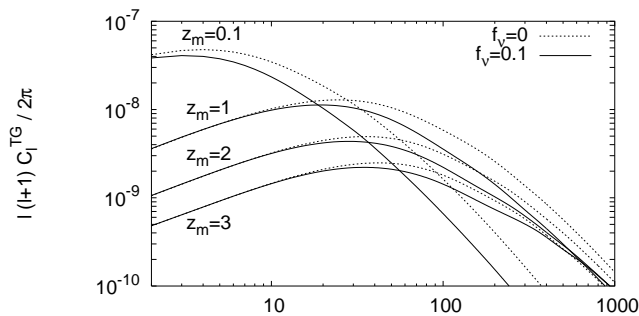


FIG. 3: Dimensionless cross-correlation spectrum in multipole space,  $l(l+1)C_l^{TG}/2\pi$ , for the same cosmological models as in Fig. 2 (i.e., with three neutrino species sharing the same mass  $m_\nu = 0$  or  $m_\nu \simeq 0.41$  eV).

$f_\nu$  for large  $l$ 's. However, we will see in Sec. II C that only the region with  $l \leq 100$  can be probed by observations: then, the neutrino-induced ISW effect is significant, but smaller than the opposite suppression effect.

In Fig. 4, we plot the corresponding angular correlation functions  $w^{TG}(\theta)$ . In this representation, the fine-structure of the high- $l$  multipole spectrum is by construction averaged out, and it is not possible to see an amplification at high  $z_m$  and small  $\theta$ . The suppression caused by neutrino masses is visible for  $z_m = 0.1$  at  $\theta \leq 15^\circ$ , and for  $z_m \geq 1$  at  $\theta \leq 2^\circ$ .

In all these plots, we used only the linear perturbation theory. Doing so, the angular cross-correlation functions depend on the matter power spectrum inside the linear regime. To prove it, we compute again  $w^{TG}(\theta)$  from the non-linear power spectrum obtained by applying HALOFIT corrections [46] to the linear one. The result, superimposed in Fig. 4, is indistinguishable from that of linear theory. This shows that non-linear effects on the evolution of matter perturbations has much less impact than that of adding a neutrino mass. This is also true for the multipoles  $C_l^{TG}$ , excepted for the smallest redshifts and highest  $l$ 's (for  $z_m = 0.1$ , non-linear effects become important for  $l > 100$ ).

### C. Detectability

For a set of full-sky CMB and LSS experiments measuring the temperature multipoles  $a_{lm}^T$  (resp. galaxy-density multipoles  $a_{lm}^G$ ) with a noise spectrum  $N_l^T$  (resp.  $N_l^G$ ), the cross-correlation spectrum  $C_l^{TG}$  can be reconstructed from the estimator

$$\tilde{C}_l^{TG} = \frac{\sum_{m=-l}^l a_{lm}^{T*} a_{lm}^G}{2l+1} \quad (12)$$

with a variance  $\sigma_l^{TG}$  given by

$$(\sigma_l^{TG})^2 = \frac{(C_l^{TG})^2 + (C_l^{TT} + N_l^{TT})(C_l^{GG} + N_l^{GG})}{2l+1}. \quad (13)$$

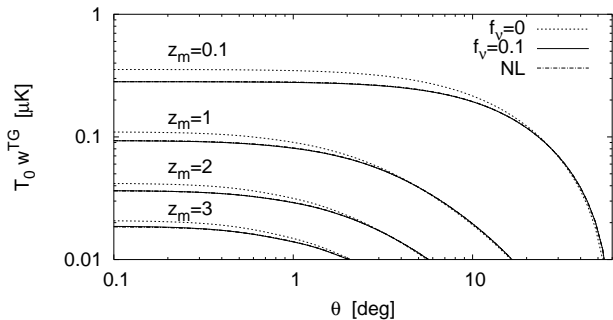


FIG. 4: Angular cross-correlation function, multiplied by the average CMB temperature and displayed in units of micro-Kelvins, for the same cosmological models as in Figs. 2,3. We also plot the same functions including non-linear (NL) corrections to the matter power spectrum: they are indistinguishable from the linear ones.

Note that the estimator is not Gaussian, especially for small  $l$ 's: so,  $\sigma_l^{TG}$  is only an estimate of the true (asymmetric) error bar on the reconstructed power spectrum. If the cross-correlation map can be reconstructed only inside a fraction  $f_{\text{sky}}$  of the full sky, in first approximation  $\sigma_l^{TG}$  should be multiplied by  $f_{\text{sky}}^{-1/2}$ . The variance is further reduced by  $\sqrt{\Delta l}$  in case of data binning with bin width ( $\Delta l$ ). Note that in this case the covariance matrix is no longer diagonal, but nevertheless using a diagonal matrix under these approximations has been shown to work well, compared to the exact treatment, if we choose an adequately large binning [47]. In practice, for the multipole range in which we are interested, the CMB noise spectrum  $N_l^{TT}$  is much smaller than  $C_l^{TT}$  for experiments like WMAP and beyond, and can be safely neglected in the above expression. For a LSS survey consisting in a catalogue of discrete objects (galaxies, clusters, etc.), the noise spectrum is usually dominated by the shot noise contribution  $N_l^{GG} \simeq 1/\bar{N}$ , where  $\bar{N}$  represents the mean number of objects per steradian. The largest ongoing/future surveys (e.g. SDSS) should reach typically the order of  $10^8$  or even  $10^9$ .

In Fig. 5, we show the typical errorbar that could be expected from a cross-correlation map with coverage  $f_{\text{sky}} = 0.65$  (corresponding to the usual galactic cut in CMB maps), using an ambitious LSS survey with surface density  $\bar{N} = 10^9 \text{st}^{-1}$  in each redshift bin. We assumed  $b(z) \sim 1$  for simplicity. These assumptions correspond essentially to the best measurement that could ever be done, since for such a high surface density the variance of the estimator of a single multipole product  $a_{lm}^{T*} a_{lm}^G$  is not affected by instrumental noise, and reduces to

$$\sigma_{lm}^{TG} = C_l^{TG} \sqrt{1 + \frac{C_l^{TT} C_l^{GG}}{(C_l^{TG})^2}}. \quad (14)$$

This expression can be interpreted as the product of the cosmic variance term  $C_l^{TG}$  times an enhancement factor depending on the correlation coefficient

$(C_l^{TG})^2 / (C_l^{TT} C_l^{GG})$ . At large  $l$ 's, the late ISW contribution to the total temperature anisotropy becomes vanishingly small, and the primary anisotropy plays the role of a large noise term, which cannot be removed. In this limit, the correlation coefficient is much smaller than one, and the variance  $\sigma_{lm}^{TG}$  gets correspondingly enhanced. Fig. 5 shows that the spectrum  $C_l^{TG}$  can be reconstructed to some extent only in the range  $l \leq 100$ ; beyond, one could only derive upper bounds. Note that the errorbar for each bin is roughly of the same order of magnitude as the effect of neutrino masses when  $f_\nu$  varies from 0 to 0.1. In Fig. 5, we also show the error degradation when  $f_{\text{sky}}$  is reduced to 0.25 and  $\bar{N}$  to  $7 \times 10^8 \text{st}^{-1}$  in each redshift bin. Finally, in Fig. 6, we plot the corresponding error bars for  $w^{TG}(\theta)$ . Note that the synthetic error bars for  $w^{TG}(\theta)$  are correlated with each other, unlike those for  $C_l^{TG}$ . On small angular scales  $\theta \leq 1$  (where the effect of neutrino masses is maximal) the  $1\sigma$  error on  $w^{TG}(\theta)$  is of the order of 25%.

We conclude from these estimates that the temperature-galaxy correlation power spectrum  $C_l^{TG}$  is potentially sensitive to the neutrino mass in the observable range  $10 < l < 100$ , as well as the angular correlation function  $w^{TG}(\theta)$  for  $\theta < 5^\circ$  at  $z = 0.5$  or  $\theta < 3^\circ$  at  $z = 1$ . Unfortunately, the enhancement of the ISW effect due to the impact of massive neutrinos on the linear growth factor is not directly visible: it would require precise data at high  $l$  and high redshift, for which the late ISW effect is masked by primordial anisotropies. The net effect of massive neutrinos on the observable part of  $C_l^{TG}$  and on  $w^{TG}(\theta)$  is a suppression, caused by the usual free-streaming effect. However this effect is non-trivial in the sense that  $C_l^{GG}$  and  $C_l^{TG}$  depend on  $f_\nu$  through different relations, due to the fact that the ISW term involves a time-derivative of the gravitational potential while the galaxy overdensity does not. Hence, the galaxy-temperature correlation spectrum can bring some information on neutrino masses which is not already contained in the sole galaxy auto-correlation spectrum. In the next section, we will quantify this statement by performing a parameter extraction from mock data accounting for future experiments.

### III. AN MCMC ANALYSIS OF MOCK DATA

For a given data set consisting in various maps (i.e. multipoles  $a_{lm}^X$ ) covering a fraction  $f_{\text{sky}}$  of the full sky and assumed to obey Gaussian statistics, the likelihood function  $\mathcal{L}$  is often approximated as

$$\mathcal{L} \propto \Pi_l \left\{ (\det C_l^{\text{th}})^{-1/2} \exp \left[ -\frac{1}{2} \text{Trace} C_l^{\text{obs}} C_l^{\text{th}^{-1}} \right] \right\}^{(2l+1)f_{\text{sky}}} \quad (15)$$

where  $C_l^{\text{obs}}$  is the data covariance matrix defined by  $[C_l^{\text{obs}}]_{XY} = \langle a_{lm}^X a_{lm}^Y \rangle$ , and  $C_l^{\text{th}}$  the assumed theoretical covariance matrix for a given fit, which contains the

sum of each theoretical power spectrum  $C_l^{XY\text{th}}$  and of the instrumental noise power spectra  $N_l^{XY}$ , estimated by modeling the experiment. Of course, the data covariance matrix reconstructed from the observed maps is also composed of signal and noise contributions. Simulating a future experimental data set amounts in computing the noise spectra  $N_l^{XY}$ , given some instrumental specifications, and generating randomly some observed spectra  $C_l^{XY\text{obs}}$ , given the theoretical spectra  $C_l^{XY\text{fid}}$  of the assumed fiducial model and the noise spectra  $N_l^{XY}$ . However, for the purpose of error forecast, it is sufficient to replace simply  $C_l^{XY\text{obs}}$  by the sum  $C_l^{XY\text{fid}} + N_l^{XY}$ : this just amounts in averaging over many possible mock data sets for the same model, and does not change the reconstructed error on model parameters [48].

For instance, if one wants to estimate future errors for a CMB experiment, the maps to consider are temperature and  $E$ -polarization:  $X \in \{T, E\}$  (here, for simplicity, we consider models with no gravitational waves and discard  $B$ -polarization). The covariance matrices then read

$$C_l^{\text{obs}} = \begin{pmatrix} C_l^{TT\text{fid}} + N_l^{TT} & C_l^{TE\text{fid}} \\ C_l^{TE\text{fid}} & C_l^{EE\text{fid}} + N_l^{EE} \end{pmatrix}, \quad (16)$$

$$C_l^{\text{th}} = \begin{pmatrix} C_l^{TT\text{th}} + N_l^{TT} & C_l^{TE\text{th}} \\ C_l^{TE\text{th}} & C_l^{EE\text{th}} + N_l^{EE} \end{pmatrix}. \quad (17)$$

Should one consider the combination of CMB data with a future galaxy redshift survey decomposed in  $N$  maps associated to  $N$  redshift bins, the matrices would become  $2 + N$  dimensional, with an extra block

$$[C_l]_{2+i,2+j} = C_l^{G_i G_j} + \delta_{ij} N_l^{G_i G_i}, \quad i = 1, \dots, N, \quad (18)$$

as well as non-diagonal coefficients  $[C_l]_{1,2+i} = C_l^{TG_i}$  accounting for the late ISW effect. Note that all non-diagonal coefficients have no noise term, since the noise contributions in two different maps are expected to be statistically uncorrelated at least at first order.

Finally, the option which is most interesting in our context, is to assume that the galaxy density auto-correlation maps are not known (or just not considered, because they could be plagued by some systematic effects), and that CMB data are only combined with the cross-correlation data, i.e. with  $N$  observed power spectra spectra  $C_l^{TG_i\text{obs}}$ . This is exactly what is being done in the current literature, in which authors try to get some new independent bounds on  $\Omega_\Lambda$  from CMB plus CMB-LSS cross-correlation data, without employing LSS auto-correlation maps. In the approximation of Gaussian-distributed  $C_l^{TG_i}$  with central value  $C_l^{TG_i\text{th}}$  and covariance given by

$$\begin{aligned} [\text{Cov}]_{ij} &\equiv \left\langle \left( C_l^{TG_i} - \langle C_l^{TG_i} \rangle \right) \left( C_l^{TG_j} - \langle C_l^{TG_j} \rangle \right) \right\rangle \\ &= \frac{C_l^{TG_i\text{th}} C_l^{TG_j\text{th}} + (C_l^{TT\text{th}} + N_l^{TT})(C_l^{G_i G_j\text{th}} + \delta_{ij} N_l^{G_i G_i})}{(2l+1)f_{\text{sky}}}, \end{aligned} \quad (19)$$

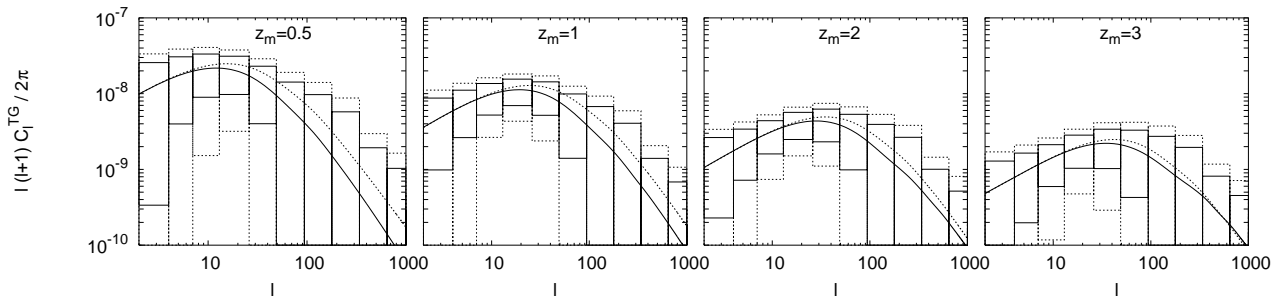


FIG. 5: 68% error forecast on the power spectrum  $C_l^{TG}$ , which is displayed for the same two cosmological models as in Figures 2, 3 (with  $f_\nu = 0$  or 0.1). The smallest error boxes assume a LSS survey with sky coverage  $f_{\text{sky}} = 0.65$  and surface density  $\bar{N} = 10^9 \text{st}^{-1}$  in each redshift bin. The binning in multipole space can be read from the width of each box. The largest error boxes correspond to  $f_{\text{sky}} 0.25$  and  $\bar{N} = 7 \times 10^8 \text{st}^{-1}$ .

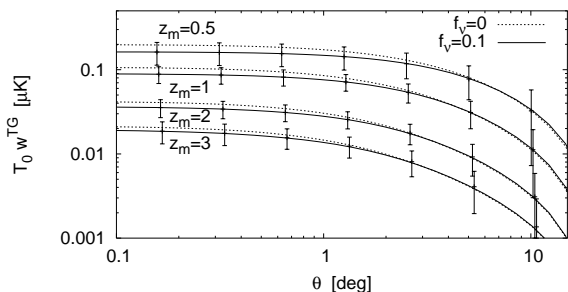


FIG. 6: 68% error forecast on the angular correlation function  $w^{TG}$ , which is displayed for the same two cosmological models as in Figures 2, 3 (with  $f_\nu = 0$  or 0.1). The error bars assume a LSS survey with sky coverage  $f_{\text{sky}} = 0.65$  and surface density  $\bar{N} = 10^9 \text{st}^{-1}$  in each redshift bin. The spacing between each error bar reflects the binning width chosen in angular space.

the likelihood of the cross-correlation data reads

$$\mathcal{L} \propto \Pi_l (\det \text{Cov}_l)^{-1/2} \exp \left[ -\frac{1}{2} \sum_{ij} \Delta_i^j [\text{Cov}_l]_{ij}^{-1} \Delta_j^i \right] \quad (20)$$

with  $\Delta_l^i \equiv C_l^{TG_i, \text{obs}} - C_l^{TG_i, \text{th}}$ . The total likelihood is then the product of the CMB and cross-correlation likelihoods.

In this section, we will focus on three ambitious future experiments: the Planck satellite, to be launched in 2008, which is expected to make the ultimate measurement of CMB temperature anisotropies, dominated by cosmic variance rather than noise up to very high  $l$ ; the Dark Energy Survey (DES); and the Large Synoptic Survey Telescope (LSST), designed primarily for a tomographic study of cosmic shear, which would provide as a byproduct a very deep and wide galaxy redshift survey (close to ideal for the purpose of measuring the CMB-LSS cross-correlation since  $N_l^{G_i G_i} < C_l^{G_i G_i}$  at least for multipoles  $l < 100$ ). For Planck, we computed the noise-noise spectra,  $N_l^{TT}$  and  $N_l^{EE}$ , like in Ref. [49], with nine frequency channels. For the DES-like survey, we followed Ref. [50]

and assumed a total number of galaxies of 250 million in a 5000 square degree area on the sky (or  $f_{\text{sky}} = 0.13$ ), with an approximate  $1\text{-}\sigma$  error of 0.1 in photometric redshifts, divided in four redshift bins with mean redshifts  $z_i \in \{0.3, 0.6, 1, 1.3\}$ , with the same selection functions as in Ref. [50]. For LSST, we used the same modeling as in [51], with a net galaxy angular number density of 80 per square arcminute and a coverage of  $f_{\text{sky}} = 0.65$ . The galaxies are divided into six redshift bins with mean redshifts  $z_i \in \{0.49, 1.14, 1.93, 2.74, 3.54, 4.35\}$ . For each bin the selection function, estimated bias  $b_i$  and galaxy density  $n_i$  are provided in [51] (Fig. 2, Eq. (16) and Table I). The noise spectra  $N_l^{G_i G_i}$  are then simply given by  $1/n_i$ .

We used the public code COSMOMC [52] to do a Monte-Carlo Markov Chain (MCMC) analysis, fitting the theoretical galaxy-temperature correlation to the mock data. For this purpose, we have written a module which computes the correlation multipoles following Eq. (4) and the likelihood of the mock data given each model as described above.

We then ran our modified version of CosmoMC for a model with eight parameters: the usual six of minimal  $\Lambda$ CDM (baryon density  $\Omega_b h^2$ , dark matter density  $\Omega_{dm} h^2$ , angular diameter of the sound horizon at last scattering  $\theta$ , optical depth to reionization  $\tau$ , primordial spectral index  $n_s$ , primordial amplitude  $\log[10^{10} A_s]$ ) plus the total neutrino mass  $m_\nu$  and the equation-of-state parameter  $w$ . Our fiducial model was close to the WMAP best-fitting model with  $m_\nu = 0$  and  $w = -1$ . We considered three possible combinations of data: Planck alone, Planck plus its cross-correlation with DES or LSST (but no information on galaxy auto-correlations), and finally Planck plus LSST, using all information and including the correlation. The probability of each parameter is displayed in Fig. 7 for each of these four cases called respectively CMB (Planck), CMB+GT (Planck+DES or Planck+LSST) and CMB+GT+GG (Planck+LSST).

Obviously the combination CMB+GT+GG does a much better job than CMB+GT for constraining all parameters (and most spectacularly  $w$  and  $m_\nu$ ). This is

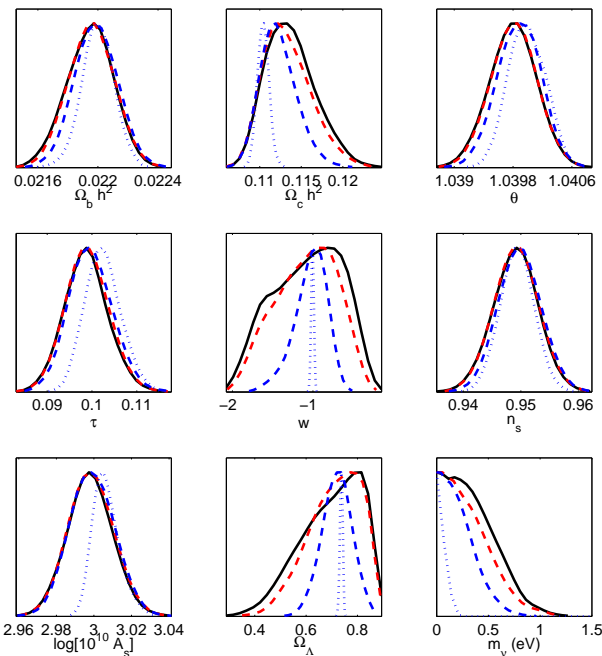


FIG. 7: Marginalized probability of cosmological parameters obtained by fitting some mock data mimicking the properties of Planck, DES and LSST. The solid black curves accounts for CMB only, the red dashed for CMB+GT with Planck+DES, the blue dashed for CMB+GT with Planck+LSST, and the dotted blue for CMB+GT+GG with Planck+LSST (these combinations are precisely defined in the text). In each of these cases the cosmological model consists in  $\Lambda$ CDM (six parameter) plus an arbitrary total neutrino mass  $m_\nu$  and equation-of-state parameter  $w$ . So, only eight of the above nine parameters are independent (as a consequence the prior for  $\Omega_\Lambda$  is non-flat). The mock data is based on a fiducial model with  $m_\nu = 0$  and  $w = -1$ .

mainly due to the fact that the GT cross-correlation is partly screened by primary temperature anisotropies, while the GG signal does not have such an intrinsic noise contribution. We even try to repeat the CMB+GT+GG analysis with all  $C_l^{GT_i}$  correlations set to zero, and found no noticeable difference, showing that most sensitivity comes from GG rather than GT terms. However, the comparison between CMB alone and CMB+GT is still interesting *per se*. In fact, we are dealing here with an idealized situation, but in the future the GG auto-correlation signal could appear to be plagued by various systematic effects. In this case, independent information coming from the cross-correlation signal alone might be a useful piece of evidence in favor of the preferred model. Also, if the galaxy bias turns out to be very difficult to estimate with high enough accuracy, one may adopt the point of view of using the GG signal to measure bias, and the CMB+GT signal to estimate the best-fit parameters in some iterative scheme.

In this perspective, it is interesting to note that the CMB+GT combination from Planck and LSST increases significantly the sensitivity of Planck alone mainly for

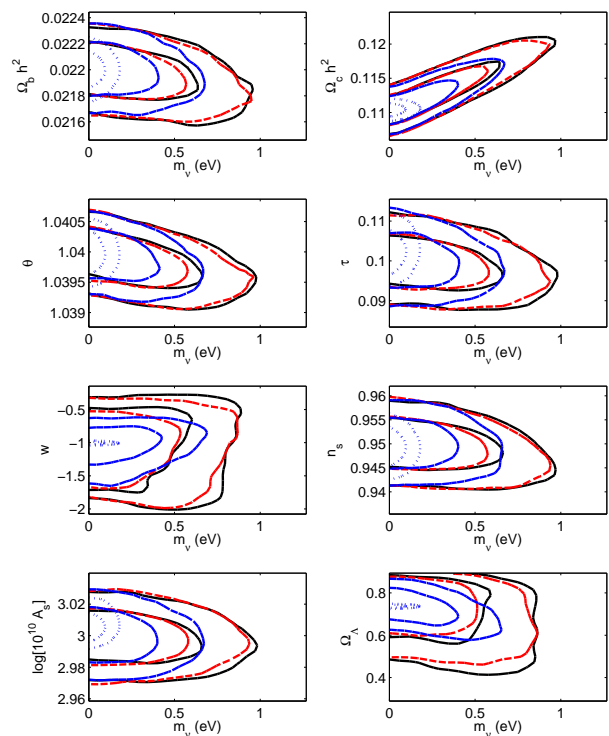


FIG. 8: Two-dimensional marginalized likelihood contours involving  $m_\nu$  obtained by fitting some mock data mimicking the properties of Planck, DES and LSST. The solid black curves accounts for CMB only, the red dashed for CMB+GT with Planck+DES, the blue dashed for CMB+GT with Planck+LSST, and the dotted blue for CMB+GT+GG with Planck+LSST (these combinations are precisely defined in the text). For each case, the two lines represent the 68% and 95% confidence levels.

$\Omega_{dm} h^2$  (by 30%),  $w$  (by 83%) and  $m_\nu$  (by 38%). As a consequence, the sensitivity to the related parameter  $\Omega_\Lambda$  increases by 76%. For our fiducial model with  $m_\nu = 0$ , the 95% confidence level upper bound on the total neutrino mass shrinks from 0.77 eV to 0.54 eV (for another fiducial model with  $m_\nu > 0$  the sensitivity can only be larger than that, see e.g. [39]). At this level of sensitivity, the parameter  $m_\nu$  is not correlated with  $\Omega_\Lambda$  or  $w$ , as can be checked by looking at two-dimensional marginalized likelihood contours in Figure 8. We conclude that the cross-correlation signal derived from Planck and LSST would have some useful sensitivity to both neutrino masses and dark energy parameters. Instead, the correlation between Planck and DES does not bring significant new information with respect to Planck alone.

Ichikawa and Takahashi [44] performed a similar forecast for Planck and LSST (with slightly different specifications), using a Fisher matrix analysis rather than MCMC approach. They find a smaller sensitivity of the cross-correlation data to neutrino mass than we do, possibly because of the various approximations entering into the Fisher matrix approach.



#### IV. CONCLUSIONS

We have studied here the possibility to use the cross-correlation between CMB and galaxy density maps as a tool for constraining the neutrino mass. On one hand massive neutrinos reduce the cross-correlation spectrum because their free-streaming slows down structure formation; on the other hand, they enhance it because of the behavior of the linear growth in presence of massive neutrinos. Using both analytic approximations and numerical computations, we showed that in the observable range of scales and redshifts, the first effect dominates, but the second one is not negligible. Hence the cross-correlation between CMB and LSS maps could bring some independent information on neutrino masses. We performed an error forecast analysis by fitting some mock data inspired from the Planck satellite, Dark Energy Survey (DES) and Large Synoptic Survey Telescope (LSST). For Planck and LSST, the inclusion of the cross-correlation data increases the sensitivity to  $m_\nu$  by 38%,  $w$  by 83% and  $\Omega_{dm}h^2$  by 30% with respect to the CMB data alone. With the fiducial model employed in this analysis (based on eight free parameters) the standard deviation for the neutrino mass is equal to 0.38 eV for Planck alone and 0.27 eV for Planck plus cross-correlation data. This is far from being as spectacular as the sensitivity expected from the measurement of the auto-correlation power spectrum of future galaxy/cluster redshift surveys or cosmic shear experiments, for which the predicted standard deviation is closer to the level of 0.02 eV, leading to a  $2\sigma$  detection even in the case of the minimal mass scenario allowed by current data on neutrino oscillations (see [38] for a review). However, the method proposed here is independent and affected by different systematics. So, it remains potentially interesting, but only if the neutrino mass is not much smaller than  $m_\nu \sim 0.2$  eV.

#### Acknowledgements

This work was initiated during a very nice and fruitful stay at the Galileo Galilei Institute for Theoretical Physics, supported by INFN. JL would like to thank Ofer Lohav for useful exchanges. The project was completed thanks to the support of the EU 6th Framework Marie Curie Research and Training network ‘‘UniverseNet’’ (MRTN-CT-2006-035863). Numerical simulations were performed on the MUST cluster at LAPP Annecy (IN2P3/CNRS and Universit  de Savoie). EG acknowledges the support from Spanish Ministerio de Cien-

cia y Tecnologia (MEC), project AYA2006-06341 with EC-FEDER funding and research project 2005SGR00728 from Generalitat de Catalunya.

#### Appendix: the Limber approximation

Let us consider some maps  $X(\hat{n})$  expanded in spherical harmonics

$$X(\hat{n}) = \sum_{l=0}^{\infty} \sum_{-l}^l a_{lm}^X Y_{lm}(\hat{n}) \quad (21)$$

with

$$a_{lm}^X = \int d^2n Y_{lm}^*(\hat{n}) X(\hat{n}). \quad (22)$$

The two-point correlation function of any two statistically isotropic quantities  $X$  and  $Y$  can be expressed in terms of the power spectrum in multipole space

$$C_l^{XY} = \langle a_{lm}^X a_{lm}^{Y*} \rangle, \quad (23)$$

or in terms of the angular correlation function in a Legendre polynomial basis ( $p_l$ )

$$w^{XY}(\theta) = \sum_l \frac{2l+1}{4\pi} p_l(\cos\theta) C_l^{XY}. \quad (24)$$

In the frame of observations, a direction dependent quantity  $X(\hat{n})$  is usually a quantity integrated over the line of sight,  $X(\hat{n}) = \int dr X(\vec{x})$ . The expression for  $a_{lm}^X$ , (22), can then easily be transformed to Fourier space. Subsequently expanding the plain wave in spherical harmonics and applying the completeness relation for spherical harmonics, one arrives at

$$a_{lm}^X = (-i)^l \int dr \frac{d^3k}{2\pi^2} X(\vec{k}) j_l(kr) Y_{lm}^*(\hat{k}), \quad (25)$$

where  $X(\vec{k})$  is the Fourier transform of  $X(\vec{x})$ ,  $j_l(r)$  is the spherical Bessel function, and  $k = |\vec{k}|$ . This expression can be simplified using Limbers approximation,  $\int dx f(x) j_l(x) \simeq \sqrt{\frac{\pi}{2l+1}} \int dx f(x) \delta(l + \frac{1}{2} - x)$ , leading to

$$a_{lm}^X \simeq (-i)^l \sqrt{\frac{\pi}{2l+1}} \int \frac{dr}{r} \frac{k^2 d\Omega_k}{2\pi^2} X(\hat{k}, k) Y_{lm}^*(\hat{k}), \quad (26)$$

separating the  $\vec{k}$  dependence of  $X$  in  $\hat{k}$  and  $k = \frac{l+\frac{1}{2}}{r}$ .

- 
- [1] R. K. Sachs and A. M. Wolfe, *Astrophys. J.* **147**, 73 (1967).  
 [2] R. G. Crittenden and N. Turok, *Phys. Rev. Lett.* **76**, 575 (1996), astro-ph/9510072.  
 [3] S. Perlmutter et al. (Supernova Cosmology Project), *As-*

- trrophys. J.* **517**, 565 (1999), astro-ph/9812133.  
 [4] A. G. Riess et al. (Supernova Search Team), *Astron. J.* **116**, 1009 (1998), astro-ph/9805201.  
 [5] D. N. Spergel et al. (WMAP), *Astrophys. J. Suppl.* **148**, 175 (2003), astro-ph/0302209.

- [6] D. N. Spergel et al. (WMAP) (2006), astro-ph/0603449.
- [7] P. Fosalba, E. Gaztanaga, and F. Castander, *ApJ* **350**, L37 (2003), astro-ph/0305468.
- [8] S. Boughn and R. Crittenden, *Nature* **427**, 45 (2004), astro-ph/0305001.
- [9] P. Fosalba and E. Gaztanaga, *Mon. Not. Roy. Astron. Soc.* **350**, L37 (2004), astro-ph/0305468.
- [10] N. Afshordi, Y.-S. Loh, and M. A. Strauss, *Phys. Rev. D* **69**, 083524 (2004), astro-ph/0308260.
- [11] N. Padmanabhan, C. M. Hirata, U. Seljak, D. J. Schlegel, J. Brinkmann, and D. P. Schneider, *Phys. Rev. D* **72**, 043525 (2005), arXiv:astro-ph/0410360.
- [12] A. Cabre, E. Gaztanaga, M. Manera, P. Fosalba, and F. Castander, *Mon. Not. Roy. Astron. Soc. Lett.* **372**, L23 (2006), astro-ph/0603690.
- [13] A. Cabre, E. Gaztanaga, M. Manera, P. Fosalba, and F. Castander (2006), astro-ph/0611046.
- [14] T. Giannantonio et al., *Phys. Rev. D* **74**, 063520 (2006), astro-ph/0607572.
- [15] J. D. McEwen, P. Vielva, M. P. Hobson, E. Martínez-González, and A. N. Lasenby, *Mon. Not. Roy. Astron. Soc. Lett.* **376**, 1211 (2007), arXiv:astro-ph/0602398.
- [16] N. Puchades, M. J. Fullana, J. V. Arnau, and D. Saez, *Mon. Not. Roy. Astron. Soc.* **370**, 1849 (2006), astro-ph/0605704.
- [17] U. Seljak and M. Zaldarriaga, *Astrophys. J.* **538**, 57 (2000), arXiv:astro-ph/9907254.
- [18] R. A. Sunyaev and Y. B. Zeldovich, *Nature (London)* **223**, 721 (1969).
- [19] N. Afshordi, Y.-T. Lin, D. Nagai, and A. J. R. Sanderson, *Mon. Not. Roy. Astron. Soc.* **378**, 293 (2007), arXiv:astro-ph/0612700.
- [20] J. R. Primack, *SLAC Beam Line* **31N3**, 50 (2001), astro-ph/0112336.
- [21] M. Maltoni, T. Schwetz, M. A. Tortola, and J. W. F. Valle, *New J. Phys.* **6**, 122 (2004), hep-ph/0405172.
- [22] G. L. Fogli, E. Lisi, A. Marrone, and A. Palazzo, *Prog. Part. Nucl. Phys.* **57**, 742 (2006), hep-ph/0506083.
- [23] A. Cuoco et al., *Int. J. Mod. Phys. A* **19**, 4431 (2004), astro-ph/0307213.
- [24] G. Steigman, *Int. J. Mod. Phys. E* **15**, 1 (2006), astro-ph/0511534.
- [25] G. Mangano, A. Melchiorri, O. Mena, G. Miele, and A. Slosar, *JCAP* **0703**, 006 (2007), astro-ph/0612150.
- [26] P. Crotty, J. Lesgourgues, and S. Pastor, *Phys. Rev. D* **67**, 123005 (2003), astro-ph/0302337.
- [27] E. Pierpaoli, *Mon. Not. Roy. Astron. Soc.* **342**, L63 (2003), astro-ph/0302465.
- [28] V. Barger, J. P. Kneller, H.-S. Lee, D. Marfatia, and G. Steigman, *Phys. Lett. B* **566**, 8 (2003), hep-ph/0305075.
- [29] R. Trotta and A. Melchiorri, *Phys. Rev. Lett.* **95**, 011305 (2005), astro-ph/0412066.
- [30] S. Hannestad, *JCAP* **0601**, 001 (2006), astro-ph/0510582.
- [31] S. Hannestad and G. G. Raffelt, *JCAP* **0611**, 016 (2006), astro-ph/0607101.
- [32] K. Ichikawa, M. Kawasaki, and F. Takahashi, *JCAP* **0705**, 007 (2007), astro-ph/0611784.
- [33] F. de Bernardis, A. Melchiorri, L. Verde, and R. Jimenez (2007), arXiv:0707.4170 [astro-ph].
- [34] J. Hamann, S. Hannestad, G. G. Raffelt, and Y. Y. Y. Wong, *JCAP* **0708**, 021 (2007), arXiv:0705.0440 [astro-ph].
- [35] J. R. Bond, G. Efstathiou, and J. Silk, *Phys. Rev. Lett.* **45**, 1980 (1980).
- [36] S. Hannestad (2007), arXiv:0710.1952 [hep-ph].
- [37] S. Hannestad, *Ann. Rev. Nucl. Part. Sci.* **56**, 137 (2006), hep-ph/0602058.
- [38] J. Lesgourgues and S. Pastor, *Phys. Rept.* **429**, 307 (2006), astro-ph/0603494.
- [39] J. Lesgourgues, S. Pastor, and L. Perotto, *Phys. Rev. D* **70**, 045016 (2004), hep-ph/0403296.
- [40] S. Wang, Z. Haiman, W. Hu, J. Khoury, and M. May, *Phys. Rev. Lett.* **95**, 011302 (2005), astro-ph/0505390.
- [41] S. Hannestad and Y. Y. Y. Wong, *JCAP* **0707**, 004 (2007), astro-ph/0703031.
- [42] Y.-S. Song and L. Knox (2003), astro-ph/0312175.
- [43] S. Hannestad, H. Tu, and Y. Y. Y. Wong, *JCAP* **0606**, 025 (2006), astro-ph/0603019.
- [44] K. Ichikawa and T. Takahashi (2005), astro-ph/0510849.
- [45] A. Kiakotou, O. Elgaroy, and O. Lahav (2007), arXiv:0709.0253 [astro-ph].
- [46] R. E. Smith et al. (The Virgo Consortium), *Mon. Not. Roy. Astron. Soc.* **341**, 1311 (2003), astro-ph/0207664.
- [47] A. Cabre, P. Fosalba, E. Gaztanaga, and M. Manera, *ArXiv Astrophysics e-prints* (2007), astro-ph/0701393.
- [48] L. Perotto, J. Lesgourgues, S. Hannestad, H. Tu, and Y. Y. Y. Wong, *JCAP* **0610**, 013 (2006), astro-ph/0606227.
- [49] J. Lesgourgues, L. Perotto, S. Pastor, and M. Piat, *Phys. Rev. D* **73**, 045021 (2006), astro-ph/0511735.
- [50] L. Pogosian, P. S. Corasaniti, C. Stephan-Otto, R. Crittenden, and R. Nichol, *Phys. Rev. D* **72**, 103519 (2005), astro-ph/0506396.
- [51] M. LoVerde, L. Hui, and E. Gaztanaga, *Phys. Rev. D* **75**, 043519 (2007), astro-ph/0611539.
- [52] A. Lewis and S. Bridle, *Phys. Rev. D* **66**, 103511 (2002), astro-ph/0205436.
- [53] M. Doran and G. Robbers, *JCAP* **0606**, 026 (2006), astro-ph/0601544.
- [54] M. Doran, G. Robbers, and C. Wetterich, *Phys. Rev. D* **75**, 023003 (2007), astro-ph/0609814.
- [55] in the case of “early Dark Energy” models, this statement can only be marginally true (see e.g. in [53, 54])